

A global model for the inductively coupled rf discharges in Ar/H₂ mixture

Abstract. This paper presents the simulation of the rf Inductively Coupled Plasma (ICP) characteristics in the Ar/H₂ mixture at low pressure, within a cylindrical stainless steel chamber. The global model used in this study and implemented on the COMSOL Multiphysics software, is elaborated under four main components: The fluid model for plasma species is associated with the electromagnetic equations for the calculation of the electric field using the magnetic vector potential. Moreover, since the plasma is weakly ionized, the properties of the neutral gas species must be taken into account by using the Navier-Stokes equation to describe the gas flow and the heat transfer equation to calculate the gas heating due to elastic collisions between electrons and neutrals. In this work, the model is first applied in order to understand the physical and chemical processes in the Ar/H₂ plasmas. The properties of plasma species in the mixture are second investigated as a function of hydrogen fraction assuming the Maxwellian electron energy distribution. The theoretical interpretations of the obtained results are also addressed in this paper.

Streszczenie. W artykule przedstawiono symulację właściwości rf plazmy sprzężonej indukcyjnie (ICP) w mieszaninie Ar / H₂ pod niskim ciśnieniem, w cylindrycznej komorze ze stali nierdzewnej. Model globalny zastosowany w tym badaniu i wdrożony w oprogramowaniu COMSOL Multiphysics jest opracowany w ramach czterech głównych komponentów: Model płynu dla form plazmy jest powiązany z równaniami elektromagnetycznymi służącymi do obliczania pola elektrycznego z wykorzystaniem potencjału wektora magnetycznego. Ponadto, ponieważ plazma jest słabo zjonizowana, należy wziąć pod uwagę właściwości obojętnych form gazu, stosując równanie Naviera-Stokesa do opisu przepływu gazu oraz równanie przenoszenia ciepła, aby obliczyć nagrzewanie gazu w wyniku zderzeń sprężystych między elektronami. W tej pracy model został po raz pierwszy zastosowany w celu zrozumienia procesów fizycznych i chemicznych zachodzących w plazmie ArH₂. (Model indukcyjnie sprzężonego wyładowania rf w mieszaninie ASr/H₂)

Keywords: inductively coupled plasma, hydrogen, Argon, gas temperature, gas follow, magnetic potential, fluid model

Słowa kluczowe: plazma sprzężona indukcyjnie, wodór, argon, temperatura gazu, śledzenie gazu, potencjał magnetyczny, model płynu

Introduction

Plasmas containing hydrogen are of topical interest for lots of technological applications like, plasma processing such as etching [1], film deposition [2-4], surface passivation, and oxide reduction. [5,6] In these applications, the active species should be responsible for surface reactions in various processes, and the hydrogen containing discharges with a high dissociation rate are required as sources of such active species. Therefore, the degree of dissociation of molecular hydrogen is considered as one of the most important parameters of hydrogen containing plasmas. [7-8]

Inductively coupled plasmas (ICP), have been widely used in the material processing because the plasma density and the ion bombarding energy at the surface can be independently controlled.

Because of their importance, there has been growing efforts to understand and to simulate the discharge processes. Therefore, the objective of this research is to understand the plasma behaviours of the inductively coupled rf discharges in Ar/H₂ using a global model. For this purpose, significant reactions among the reactive species in the discharge, electrons, ions, and atoms must be taken into account, including the effects of the plasma-wall interactions. In particular, reactions of metastable-state species play a key role in determining the plasma properties because these metastable-state species possess unusual properties, and a large fraction of the ground-state atoms exist in the metastable-state in low-pressure high-density plasmas, which phenomenon is extensively exploited in modern semiconductor and display industries. [13,14]

The model used in this study to simulate the inductively coupled rf discharge takes into account the important effect of neutral species on the plasma properties, this is reflected by the description of their characteristics which are temperature by the use of the heat transfer equation and gas flux by the Navier-stocks equation, these equations are coupled to the fluid model equations for the plasma species and the electromagnetic equations for the electric field.

In this paper, the global model for rf inductively-coupled discharge is first applied in order to understand the physical and chemical processes in the Ar/H₂ plasmas. The properties of plasma species in the mixture are second investigated as a function of hydrogen fraction.

Description of the model

A schematic diagram of the reactor for inductively coupled rf discharge to be modelled is shown in Fig. 1. The reactor is considered cylindrical and perfectly axisymmetric. It consists of a cylindrical stainless steel chamber with an inner radius of 80 mm and height of 75 mm. A quartz plate of 10 mm thickness is placed at the upper end of the chamber. The discharge is sustained by the electric field induced by a variable magnetic field, this is due to the circulation of a high frequency current (13.56 Mhz) in a coil mounted about 5 mm above the quartz plate. The coil is perfectly concentric in the center of the chamber to maintain the discharge symmetry.

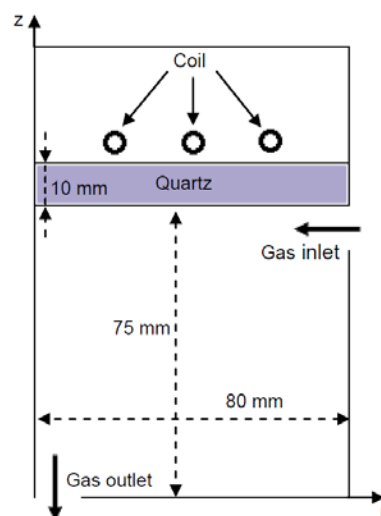


Fig.1. Schematic diagram of the ICP reactor

Model equations

The model equations considered in this study to describe the behaviours of the inductively coupled rf discharge in Ar/H₂ mixture are described below.

Electromagnetic equations

In the case of the axisymmetric inductive coupling plasma model, Maxwell's electromagnetic field equations can be reduced to the potential vector A as follows:

$$(1) \quad \frac{1}{\mu_0 \mu_r} \nabla^2 A + \varepsilon_0 \varepsilon_r \omega_{rf}^2 A = -J$$

where J is the current density in the coil, while J is complex, $\text{Im}(J)$ could be set to zero.

Solving this equation gives the electromagnetic distribution of the vector potential A in the computational domain. Only the values obtained in the plasma environment are useful for coupling with the electron energy equation through the electric field and the mean value of the power density deposited in the plasma.

These two quantities can be calculated by the following relations:

$$(2) \quad E = -\nabla V - \frac{\partial A}{\partial t}$$

$$(3) \quad P_{ind} = \frac{1}{2} R_e(\sigma_p) \omega_{rf}^2 |A|^2$$

where, V is the electric potential and σ_p is the complex conductivity of the plasma, it is given by the following expression:

$$(4) \quad \sigma_p = \frac{n_e e^2}{m_e (v_{en} + j \omega_{rf})}$$

where, m_e , v_{en} and e represent respectively the electronic mass and the effective momentum transfer collision frequency and the elementary charge. The dielectric constant of the plasma is obtained from the following relation:

$$(5) \quad \varepsilon_p = \varepsilon_0 \left(1 - j \frac{\sigma_p}{\varepsilon_0 \omega_{rf}} \right)$$

Gas flow Equation

Neutral species have an important influence on the distribution of plasma through two aspects:

- The source / loss where the plasma generates or dissipates is proportional to the density of the neutral gas;
- The density of the neutral gas can change the collision frequency of electrons and other particles.

Considering the influence of the neutral gas and the pressure distribution on the plasma in this model, the flux of the neutral gas is described by the incompressible Navier-Stokes equation.

$$(6) \quad \rho \frac{\partial u}{\partial t} - \nabla \eta (\nabla u + (\nabla u)^T) + \rho u \nabla u + \nabla p = F$$

$$(7) \quad \nabla u = 0$$

where ρ , η and u represent respectively the gas density, the dynamic viscosity and the velocity vector, p is the gas pressure and F is the force. In this case, the force is zero.

1.3 Heat transfer equation

Generally, low pressure discharges are characterized by the fact that the temperature of the electron is much higher than the neutral gas temperature due to the low collision

frequency. In the inductively coupled plasmas, which are characterized by a high ionization rate and collision frequency, therefore the neutral species are heated. The cooling of these neutrals is caused by the reaction with the walls of the reactor. Generally, the temperature in the reactor is not uniform, and this subsequently influences the pressure of the neutrals and the distribution of the plasma species. The conservation of the heat energy in the reactor is governed by the Fourier equation expressed as follows:

$$(8) \quad \rho C_p \frac{\partial T}{\partial t} + \rho C_p u \nabla T + \nabla(-K \nabla T) = Q$$

where T is the temperature, K , C_p and Q are respectively the thermal conductivity, the specific heat capacity at constant pressure and the heat source term.

Plasma species Equations

In fluid models, each species is treated as a separate fluid to satisfy the conservation of mass over the entire computational domain. For electrons, a Maxwellian distribution is considered. This model is based on the first three moments resolution of the Boltzmann equation. These three moments are continuity, momentum transfer and energy equations, which are strongly coupled with the Poisson's equation relating the space charge to the electrostatic potential for the inductively coupled discharges.

The continuity equation and electron momentum are given by the following equations:

$$(9) \quad \frac{\partial n_e}{\partial t} + \nabla \Gamma_e = S_e$$

$$(10) \quad \frac{\partial \left(\frac{3}{2} n_e k_B T_e \right)}{\partial t} + \nabla \Gamma_e + e \Gamma_e E = P_{ind} + W_e$$

where the flux of electrons is given by the following relation:

$$(11) \quad \Gamma_e = -n_e \mu_e E - \frac{1}{m_e v_{en}} \nabla (n_e k_B T_e)$$

And the flux of electron energy is given by the following equation:

$$(12) \quad \Gamma_e = \frac{5}{2} \left[\Gamma_e k_B T_e \frac{n_e k_B T_e}{m_e v_{en}} \nabla (n_e k_B T_e) \right]$$

Here n_e is the electron density, μ_e is the electron mobility, T_e is the electron temperature, E is the electric field vector, k_B is the Boltzmann constant and S_e is the source term of the electrons.

The inductive heating term P_{ind} is obtained from the electromagnetic model. The term W_e represents the transfer of mass and energy to the electrons by collisions with another species of density N_k , it is given by the following relation:

$$(13) \quad W_e = \sum_k \sum_j k_{k,j} n_e N_k \Delta \varepsilon_{k,j}$$

The continuity and momentum equations for ions are given as follows:

$$(14) \quad \frac{\partial n_i}{\partial t} + \nabla (n_i u_i) = S_i$$

$$(15) \quad \frac{\partial (n_i m_i u_i)}{\partial t} + \nabla (n_i m_i u_i) = \nabla (n_i k_B T_i) + Z_i e n_i E + M_i$$

Here n_i , u_i , S_i , m_i and Z_i are respectively the density, the velocity vector, the source term, the mass and the charge of the ions; T_i is the temperature of the ions, and M_i is the collisional transfer of the momentum of the ions to the neutral species

Neutral transport in the ground state or in the excited state is governed by the following equation:

$$(16) \quad \frac{\partial n_*}{\partial t} + \nabla(-D_* \nabla n_*) = S_*$$

where n_* , D_* , and S_* represent respectively the density, the diffusion coefficient, and the neutrals source term.

The electric field due to the space charge in the plasma and the electric field of the inductive power coupling are treated separately. The electrostatic potential is obtained by solving the Poisson equation:

$$(17) \quad \nabla^2 V = \frac{e}{\epsilon_0} (n_e - \sum_i Z_i n_i)$$

where, Z_i is the charge of the ions.

Boundary conditions

– Electric and magnetic potentials: The reactor walls are considered perfectly conductive and connected to ground, this implies that the electric potential and the vector magnetic potential are zero at the metal walls, at the level of the dielectric walls, the electric potential can be obtained by considering the following condition:

$$(18) \quad \frac{\partial \sigma_s}{\partial t} = n J_i + n J_e$$

$$(19) \quad -n(D_p - D_d) = \sigma_s$$

With σ_s , n , J_i , J_e , D_p , and D_d are, respectively, the charge accumulated on the surface of the dielectric, the surface norm, the ion current density, the electronic current density, and the electric displacement vectors in the plasma side and in the dielectric side.

– Density, flux and energy species: The electron flux at the walls and electrodes is obtained by using the boundary condition of a Maxwellian flux as follow:

$$(20) \quad \Gamma = \pm \frac{1}{4} n_e v_{e,th} e^{\frac{V}{k_B T_e}}$$

$$(21) \quad v_{e,th} = \sqrt{\frac{8k_B T_e}{\pi m_e}}$$

where the signs \pm correspond to the direction of the electron flux, V is the potential of the wall, $v_{e,th}$ is the electron thermal velocity.

Ignoring the thermal conduction of electrons, the energy flux to the electrodes and the walls is given by:

$$(22) \quad \Gamma_\varepsilon = \frac{5}{2} n_e T_e \Gamma_e$$

The ion density and velocity gradients are set to zero at the limits:

$$(23) \quad \nabla n_i = 0, \quad \nabla v_i = 0$$

- Gas temperature: the heat equation is solved by considering the Neumann condition.
- Gas flow: the Navier-Stokes equation is solved taking into account as boundary conditions, the gas velocity at the reactor inlet, zero velocity at the walls and

electrodes, and a constant pressure at the reactor outlet.

Model input parameters

The reactions considered in our study are listed in the table 1.

For electrons; mobility is calculated from their cross section and the diffusion coefficient is calculated by the Einstein relation which relates the mobility to the diffusion coefficient.

The ions mobility is calculated by the Dalgarno relation [41] by taking a long-range polarization interaction potential, and the diffusion coefficient is determined by the Einstein relation.

$$(24) \quad \mu_i = \frac{36}{\sqrt{\alpha_n m_r}} \frac{2.69 \times 10^{25}}{N}$$

$$(25) \quad \frac{D_i}{\mu_i} = \frac{k_B T_i}{q_i}$$

where N is the gas density, q_i is the charge of the ion, μ_i is the mobility, m_r is the reduced ion-neutral mass, α_n is the polarizability in function a_0^3 (a_0 is the Bohr radius), D_i is the ionic diffusion coefficient, k_B is the Boltzmann constant, and T_i is the ionic temperature.

The diffusion coefficient of the excited particles is calculated taking into account a Lennard-Jones type interaction potential.

$$(26) \quad D_* = 0.0018583 \sqrt{\frac{T^3}{m_r}} \frac{1}{p \sigma_{EN}^2 \Omega_D}$$

$$(27) \quad \Omega_D = \frac{1.06036}{\Psi^B} + \frac{0.193}{e^{D\Psi}} + \frac{1.03587}{e^{F\Psi}} + \frac{1.76464}{e^{H\Psi}}$$

$$(28) \quad \sigma_{EN} = \frac{\sigma_E + \sigma_N}{2}, \quad \Psi = \frac{T}{\sigma_{EN}}, \quad \varepsilon_{EN} = \sqrt{\varepsilon_E \varepsilon_N}$$

where T and p are the gas temperature and the pressure, m_r is the reduced mass, (σ_E , ε_E) et (σ_N , ε_N) are respectively the parameters of Leonard-Jones potential of the excited particle E and the ground state particle N . B , D , F and H are constants given by:

$$B = 0.15610, D = 0.47635, F = 1.52996, \text{ and } H = 3.89411.$$

The reaction rate with the walls and the electrodes can be calculated as follows:

$$(29) \quad k_* = \frac{D_*}{\Lambda^2}$$

For a reactor of radius R and height L , the effective diffusion length Λ can be expressed from the following relation:

$$(30) \quad \Lambda^2 = \left[\left(\frac{\pi}{L} \right)^2 + \left(\frac{2.405}{R} \right)^2 \right]^{-1}$$

Results and discussions

Some of the results obtained from the resolution of the governing equations of the global model described previously for the simulation of the inductively coupled radiofrequency plasma (ICP), are presented in this paper. The reactor is powered by a rf source (13.6 Mhz) at a power of 350 W. The gas used is composed of a mixture of hydrogen and argon with proportions of 30% and 70% respectively at pressure $p=20$ mTorr. The flow rate of the mixture is considered equal to 35 sccm.

Table.1. Reactions set for Argon (Ar), for hydrogen (H₂) and for Argon/Hydrogen mixture (Ar/H₂)

Reaction	Rate coefficient (m ³ .s ⁻¹) or (s ⁻¹)	Reference
e + H ₂ → e + H ₂ (Elastic)	σ(ε)	[15]
e + H ₂ → e + H ₂ (j=0→2,1→3,2→4,3→5)	σ(ε)	[16]
e + H ₂ → e + H ₂ (v=1,2,3)	σ(ε)	[17]
e + H ₂ → H + H ⁺	σ(ε)	[15]
e + H ₂ → e + H ₂ (triplet) → e + H + H	σ(ε)	[15]
e + H ₂ → e + H ₂ (single) → e + H ₂ + hν	σ(ε)	[15]
e + H ₂ → e + H + H(2s)	σ(ε)	[16]
e + H ₂ → e + H + H(2p)	σ(ε)	[16]
e + H ₂ → e + H + H(n=3,4,5)	σ(ε)	[16]
e + H ₂ → 2e + H ₂ ⁺	σ(ε)	[17]
e + H ₂ → 2e + H ⁺ + H	σ(ε)	[17]
e + H → e + H	σ(ε)	[16]
e + H ↔ e + H(2p)	σ(ε)	[16]
e + H ↔ e + H(2s)	σ(ε)	[16]
e + H ↔ e + H(n=3,4,5)	σ(ε)	[16]
e + H → 2e + H ⁺	σ(ε)	[16]
e + H(2p) ↔ e + H(2s)	σ(ε)	[18]
e + H(2p) → 2e + H ⁺	σ(ε)	[18]
e + H(2s) → 2e + H ⁺	σ(ε)	[18]
e + H(n=3,4,5) → 2e + H ⁺	σ(ε)	[18]
e + Ar → e + Ar (Elastic)	σ(ε)	[19]
e + Ar ↔ e + Ar ^m (4s)	σ(ε)	[19]
e + Ar ↔ e + Ar ^r (4s)	σ(ε)	[19]
e + Ar ↔ e + Ar(4p)	σ(ε)	[19]
e + Ar ↔ e + Ar(3d)	σ(ε)	[19]
e + Ar ↔ e + Ar(hl)	σ(ε)	[19]
e + Ar ^m (4s) → e + Ar ^r (4s)	k=3.7×10 ⁻¹⁴	[20]
e + Ar ^r (4s) → e + Ar ^m (4s)	k=9.1×10 ⁻¹³	[20]
e + Ar → 2e + Ar ⁺	σ(ε)	[19]
e + Ar ^m (4s) → 2e + Ar ⁺	σ(ε)	[21]
e + Ar ^r (4s) → 2e + Ar ⁺	σ(ε)	[21]
e + Ar(4p) → 2e + Ar ⁺	σ(ε)	[21]
e + Ar(3d) → 2e + Ar ⁺	σ(ε)	[21]
e + Ar(hl) → 2e + Ar ⁺	σ(ε)	[21]
e + H ⁺ → 2e + H	σ(ε)	[22]
e + H ₂ ⁺ → H ⁺ + H	σ(ε)	[18]
e + H ₃ ⁺ → e + H ⁺ + 2H	σ(ε)	[18]
e + H ₃ ⁺ → 3H	σ(ε)	[23]
e + H ₃ ⁺ → H + H ₂	σ(ε)	[23]
e + ArH ⁺ → Ar + H	k = 10 ⁻¹³	[24]
e + Ar ⁺ → Ar ^m (4s) + hν	k = 10 ⁻¹⁷	[25]
Ar ⁺ + H ₂ → ArH ⁺ + H	k=2.34T ^{0.16} ×10 ⁻¹⁶	[26]
Ar ⁺ + H ₂ → Ar + H ₂ ⁺	k=0.335T ^{0.16} ×10 ⁻¹⁶	[26]
Ar ⁺ + H → Ar + H ⁺	k=5×10 ⁻¹⁶	[27]
H ₂ ⁺ + Ar → ArH ⁺ + H	k=20.703T ^{-0.0203} exp(-2.1434/T)×10 ⁻¹⁶	[26]
H ₂ ⁺ + Ar → Ar ⁺ + H ₂	k=2.71×10 ⁻¹⁶	[26]
H ₂ ⁺ + H ₂ → H ₃ ⁺ + H	k=23.5×10 ⁻¹⁶	[26]
H ₂ ⁺ + H → H ₂ + H ⁺	k=6.4×10 ⁻¹⁶	[28]
ArH ⁺ + H ₂ → Ar + H ₃ ⁺	k=15×10 ⁻¹⁶	[29]
H ⁺ + H → e + H ₂	k=67T ^{-0.2} exp(176/T)×10 ⁻¹⁶	[30]
H ⁺ + H ⁺ → H + H(n ≥ 2)	k=2.217T ^{-0.5} ×10 ⁻¹²	[24]
H ⁺ + H ₂ ⁺ → 3H	k=1.44T ^{-0.5} ×10 ⁻¹¹	[24]
H ⁺ + H ₃ ⁺ → 4H	k=1.44T ^{-0.5} ×10 ⁻¹¹	[24]
H ⁺ + Ar ⁺ → H + Ar	k=1.3T ^{-0.5} ×10 ⁻¹²	[31]
H ⁺ + ArH ⁺ → H ₂ + Ar	k=5×10 ⁻¹²	[24]
Ar(4s) + Ar(4s,4p) → Ar + Ar ⁺	k=0.288T ^{0.5} ×10 ⁻¹²	[32,33]
Ar(4s) + Ar(3d,hl) → Ar + Ar ⁺	k=0.404T ^{0.5} ×10 ⁻¹²	[32,33]
Ar(4p,3d,hl) + Ar(4p,3d,hl) → Ar + Ar ⁺	k=0.404T ^{0.5} ×10 ⁻¹²	[32,33]
Ar ^m (4s) + Ar → 2Ar	k=2.1×10 ⁻²¹	[24]
Ar(4s,4p,3d,hl) + H ₂ → Ar + H + H	k=1.1×10 ⁻¹⁶	[34]
Ar(4s,4p,3d,hl) + H → Ar + H(2p)	k=2×10 ⁻¹⁶	[35]
Ar ^r (4s) → Ar + hν	k=0.72×10 ⁴	[36]
Ar(4p) → Ar ^m (4s) + hν	k=4.2×10 ⁷	[37]
Ar(4p) → Ar ^r (4s) + hν	k=4×10 ⁷	[37]
Ar(3d) → Ar(4p) + hν	k=6×10 ⁷	[37]
Ar(hl) → Ar ^m (4s) + hν	k=4.6×10 ⁵	[37]
Ar(hl) → Ar ^r (4s) + hν	k=1.32×10 ⁶	[37]
Ar(hl) → Ar(4p) + hν	k=2.4×10 ⁶	[37]
Ar(hl) → Ar(3d) + hν	k=3.7×10 ⁵	[37]
H(2s) + Ar → H(2p) + Ar	k=35×10 ⁻¹⁶	[38]
H(2s,2p) + H ₂ → H + H ₂ + hν	k=27×10 ⁻¹⁶	[39]
H(2s,2p) + H ₂ → 3H	k=4.5×10 ⁻¹⁶	[39]
H(2s,2p) + H ₂ → e + H ₃ ⁺	k=13.5×10 ⁻¹⁶	[39]
H(2p) → H + hν	k=4.7×10 ⁷	[9]
H(n=3) → 0.87H(2p) + 0.13H(2s) + hν	k=4.41×10 ⁷	[40]
H(n=4) → 0.87H(2p) + 0.13H(2s) + hν	k=8.42×10 ⁶	[40]
H(n=4) → H(n=3) + hν	k=8.98×10 ⁶	[40]
H(n=5) → 0.87H(2p) + 0.13H(2s) + hν	k=2.53×10 ⁶	[40]
H(n=5) → H(n=3) + hν	k=2.2×10 ⁶	[40]
H(n=5) → H(n=4) + hν	k=2.7×10 ⁶	[40]

The spatial variation of the velocity of gas flow in the reactor is shown in Fig. 2. It clearly shows that speed is very important at the outlet of the reactor than other regions because of the approximation of the speed lines at the outlet. According to the fluid mechanics laws, a reduction in section implies an increase in speed.

The distribution of the gas temperature in the plasma reactor is illustrated in fig. 3, it is obtained by solving the heat transfer equation. The temperature is very important at the center of the reactor (around 595 K) than in the vicinity of the walls because of the heat exchange with the outside environment at ambient temperature.

Fig. 4 illustrates the magnetic potential module created by the coil; the electric field induced by the temporal variation of this potential is the source of energy which will be recovered by the electrons to maintain the electric discharge.

Fig. 5, shows clearly that the value of the electrical potential in inductively coupled discharges is low, not reaching 20.9 V in our case study.

The heating of the electrons is mainly due to the electric field induced by the temporal variation of the magnetic potential, so it is logical that the spatial variation of the electronic temperature follows the variation of the vector potential; this is what appears in the fig. 6.

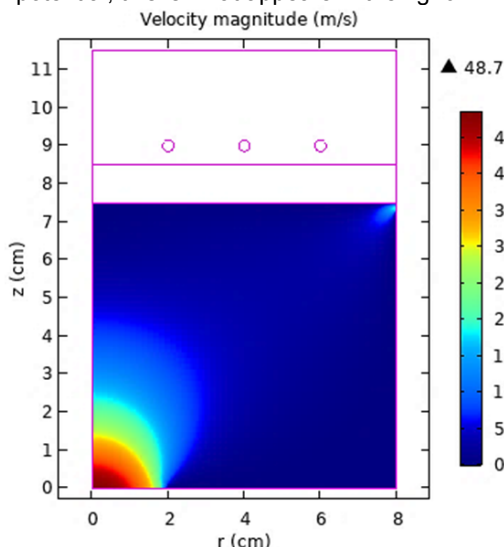


Fig. 2 Spatial distribution of the gas velocity [$m.s^{-1}$]

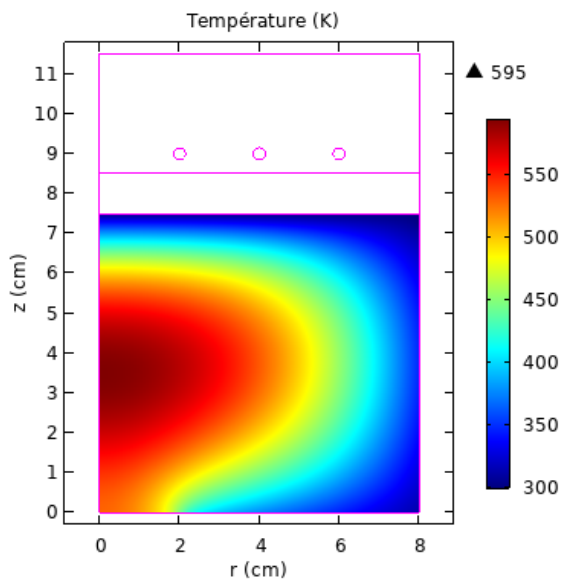


Fig. 3 Spatial distribution of the gas temperature [K]

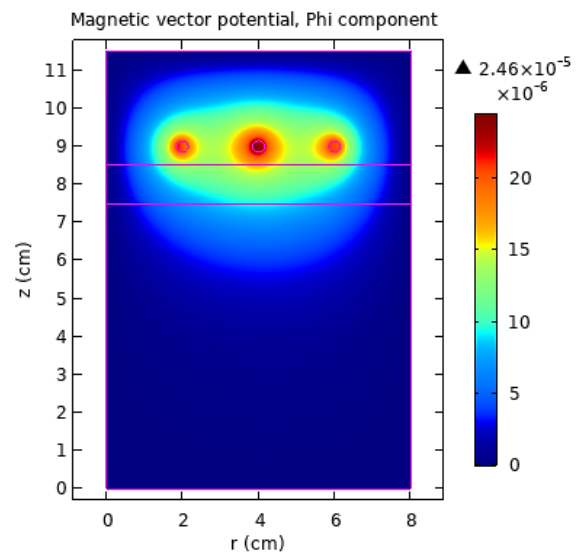


Fig. 4 Spatial distribution of the magnetic potential [$V.s.m^{-1}$]

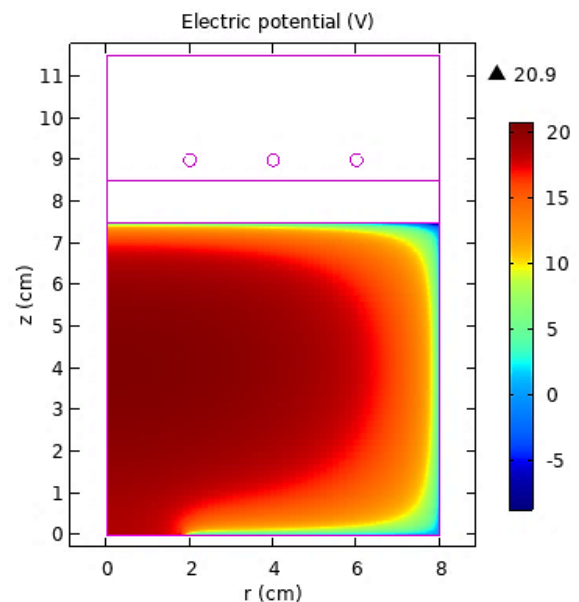


Fig. 5 Spatial distribution of the electric potential [V]

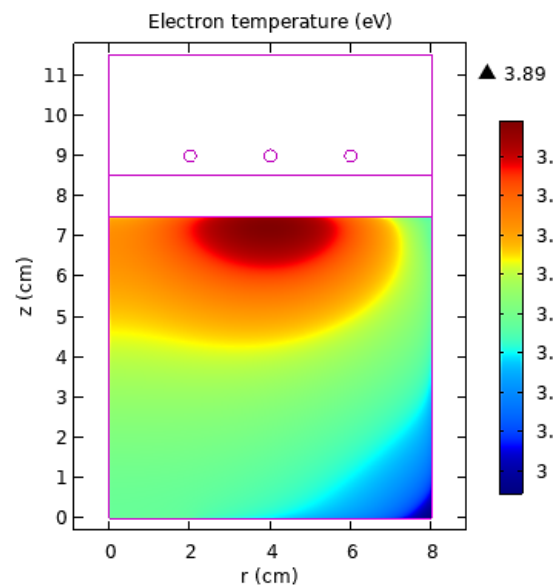


Fig. 6 Spatial distribution of the electron's temperature [eV]

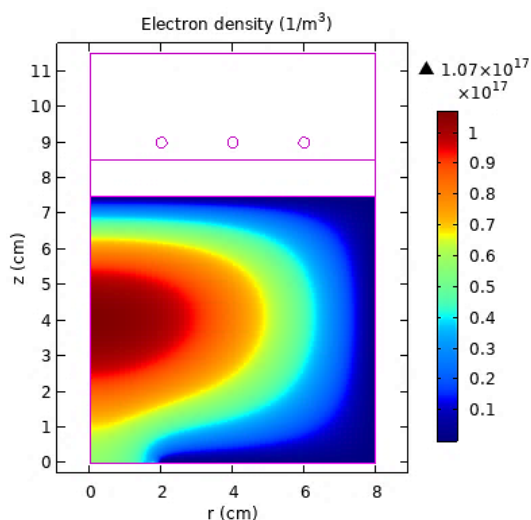


Fig. 7 Spatial distribution of the electron's density [m^{-3}]
 In inductively coupled discharges, the electron density is very important because of the confinement of the electrons by the magnetic field; under our conditions it is of the order of $1.07 \times 10^{17} \text{ cm}^{-3}$ (see Fig. 7).

In the following, some plasma parameters in inductive coupled Ar/H₂ discharges are studied as a function of the hydrogen fraction FH₂.

In Figs. 8 and 9, the electron density n_e and its temperatures T_e are shown as a function of hydrogen fraction FH₂ in the mixture Ar/H₂. The calculated n_e markedly decrease with increasing H₂.

The calculated electron temperature T_e relatively abruptly increases with increasing FH₂, until FH₂ reaches approximately 10%. For FH₂ higher than 10%, T_e gradually increases with the increase in FH₂.

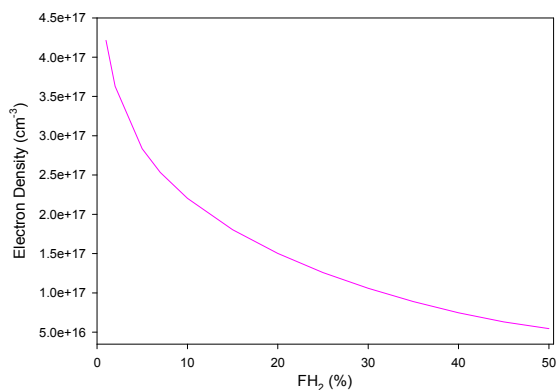


Fig. 8. Electrons density as a function of hydrogen fraction

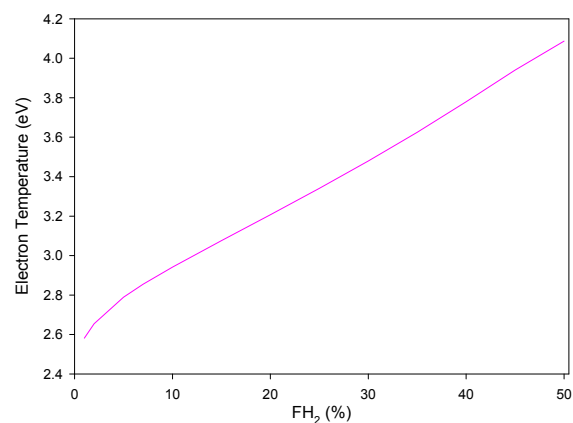


Fig. 9 Electrons temperature as a function of hydrogen fraction

The calculated positive ions densities are shown in Fig. 10. The density of Ar⁺ markedly decrease with the increase in the hydrogen fractions FH₂ owing to the charge exchange collisions between Ar⁺ and molecular hydrogens. On the other hand, the density of ArH⁺ ions abruptly increase at the hydrogen fractions lower than 5% – 10%, and then gradually decreases with the increase in the hydrogen fraction. The density of H₃⁺ relatively abruptly increases at the hydrogen fractions of approximately 10% – 20% and then does not strongly depend on the hydrogen fractions. The densities of H⁺ and particularly H₂⁺ ions are not sensitive to the hydrogen fraction at the fractions higher than 20%.

The dominant ion for all the hydrogen fractions FH₂ presented in the figure remains Ar⁺, this shows that the rate of production of this ion is greater than the rate of loss due to the reaction: $\text{Ar}^+ + \text{H}_2 \rightarrow \text{H} + \text{ArH}^+$

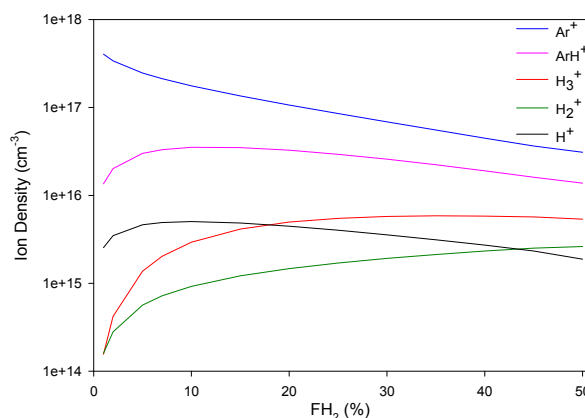


Fig. 10 Positive ions densities as a function of hydrogen Fraction

Conclusion

In conclusion, the physical and chemical behaviours of Ar/H₂ inductively coupled plasmas (ICP) was investigated in this paper by using a global model implemented in the COMSOL platform. This model considers the important effect of neutral species on the plasma parameters, as the gas temperature and his flux. The properties of plasma species are second studied as a function of hydrogen fraction in the Ar/H₂ mixture.

From the results obtained above, we can say that the global model used is able to describe correctly the electrical and physical properties of inductively coupled discharges, object of our study. For example, the gas has a very high temperature at the center of the reactor, the electrical potential is low and the electron density is very important.

The primary ions H₂⁺ and Ar⁺ which are produced by ionization of the background gas by electron collisions are effectively converted into H₃⁺ and ArH⁺. The Ar-containing ions (Ar⁺ and ArH⁺) constitute a much higher plasma density than the ions containing only H (H⁺, H₂⁺, H₃⁺). This is dominantly due to the much higher loss of H_x⁺ ions to the walls due to their lower mass. With the increase in the hydrogen fractions (FH₂): The density of Ar⁺ significantly decrease, the H₃⁺ density relatively abruptly increases at FH₂ of approximately 10% – 20% and then does not strongly depend on the hydrogen fractions, the density of ArH⁺ ions abruptly increase at FH₂ lower than 5% – 10%, and then gradually decreases. The densities of H⁺ and particularly H₂⁺ ions are not sensitive to the hydrogen fraction at the fractions higher than 15% – 20%. Therefore, it can be concluded that the addition of argon to the hydrogen discharges makes it possible to easily produce

stable plasmas, keeping the densities of H^+ , H_2^+ and H_3^+ ions over a wide range of Argon dilution.

Authors

Hocine Tebani was born in Tissemsilt, Algeria, on April, 12, 1980. His scientific interests include the theoretical study and modeling of physical processes in gas discharge plasma. He is currently a teacher researcher at University of Hassiba Ben Bouali Chlef, Algeria.

E-mail: hocinetebani@yahoo.fr

Djillali Benyoucef was born in Algeria. He is currently a Professor at University of Hassiba Benbouali of Chlef, Algeria. His field of expertise is more particularly the plasmas modeling. He has also a good expertise on the swarm parameters determination of the charged particles in non equilibrium reactive plasma.

E-mail: ben_plasma@yahoo.fr

REFERENCES

- [1] A. Efremov, N. Min, J. Jeong, Y. Kim, and K. Kwon. "Etching characteristics of Pb (Zr,Ti)O₃, Pt, SiO₂, and Si₃N₄ in an inductively coupled HBr/Ar plasma". *Plasma Sources Sci. Technol.* 19 (2010), 045020
- [2] S. Yoon, K. Tan, Rusli, and J. Ahn. "Modeling and analysis of hydrogen methane plasma in electron cyclotron resonance chemical vapor deposition of diamond-like carbon". *J. Appl. Phys.* 91 (2002). 40: 47
- [3] I. B. Denysenko, S. Xu, J. D. Long, R. P. Rutkevych, N. A. Azarenkov, and K. Ostrikov. "Inductively coupled Ar/CH₄/H₂ plasmas for low temperature deposition of ordered carbon nanostructures". *J. Appl. Phys.* 95 (2004), 2713.
- [4] J. Zhou, I. T. Martin, R. Ayers, E. Adams, D. Liu, and E. R. Fisher. "Investigation of inductively coupled Ar and CH₄/Ar plasmas and the effect of ion energy on DLC film properties". *Plasma Sources Sci. Technol.* 15 (2006), 714: 726.
- [5] J. D. Bernstein, S. Qing, C. Chan, and T.-J. King. "High dose-rate hydrogen passivation of polycrystalline silicon CMOS TFTs by plasma ion implantation". *IEEE Trans. Electron Devices* 43 (1996), 1876: 1882
- [6] M. Sode, T. Schwarz-Selinger, and W. Jacob. "Ion chemistry in H₂-Ar low temperature plasmas". *Journal of Applied Physics* 114 (2013), 063302
- [7] B. P. Lavrov, A. V. Pipa, and J. Ropcke. *Plasma Sources Sci. Technol.* 15 (2006), 135
- [8] M. Abdel-Rahman, V. Schulz-von der Gathen, T. Gans, K. Niemi, and H. F. Dobeles. *Plasma Sources Sci. Technol.* 15 (2006), 620
- [9] Kimura, Takashi, and Hiroki Kasugai. "Properties of inductively coupled rf Ar/H₂ plasmas: Experiment and global model." *Journal of Applied Physics* 107.8 (2010): 083308.
- [10] C.-F. Yeh, T.-J. Chen, C. Liu, J. Gudmundsson, and M. Lieberman, "Hydrogenation of polysilicon thin-film transistor in a planar inductive H₂/Ar discharge". *IEEE Electron Device Lett.* 20 (1999), 223:225
- [11] N. Fox-Lyon, G. S. Oehrlein, N. Ning, and D. B. Graves, "Hydrogenation and surface density changes in hydrocarbon films during erosion using Ar/ H₂ plasmas". *J. Appl. Phys.* 110 (2011), 104314
- [12] V. S. Voitsenya, D. I. Naidenkova, Y. Kubota, S. Masuzaki, A. Sagara, and K. Yamazaki, "On the possibility to increase efficiency of conditioning of vacuum surfaces by using a discharge in a hydrogen-noble gas mixture,". *Natl. Inst. Fusion Sci.* 799 (2004), 1
- [13] M. Park, H.-Y. Chang, S.-J. You, J.-H. Kim, and Y.-H. Shin, *Phys. Plasmas* 18 (2011), 103510
- [14] B. H. Seo, J. H. Kim, and S. J. You, "Effects of argon gas pressure on its metastable-state density in high-density plasmas". *Physics of Plasmas* 22 (2015), 053514
- [15] www.lxcat.net/Phelps visited 19 March 2020
- [16] L.L. Alves, "The IST-Lisbon database on LXCat" *J. Phys. Conf. Series* (2014), 565, 1
- [17] Yoon, Jung-Sik, et al. "Cross sections for electron collisions with hydrogen molecules." *Journal of Physical and Chemical Reference Data* 37.2 (2008): 913-931.
- [18] <https://www-amdis.iaea.org/ALADDIN/collision.html> visited 19 March 2020
- [19] www.lxcat.net/Hayashi visited 19 March 2020
- [20] Ferreira, C. M., J. Loureiro, and A. Ricard. "Populations in the metastable and the resonance levels of argon and stepwise ionization effects in a low-pressure argon positive column." *Journal of applied physics* 57.1 (1985): 82-90.
- [21] Hyman, H. A. "Electron-impact ionization cross sections for excited states of the rare gases (Ne, Ar, Kr, Xe), cadmium, and mercury." *Physical Review A* 20.3 (1979): 855.
- [22] Peart, B., D. S. Walton, and K. T. Dolder. "Electron detachment from H-ions by electron impact." *Journal of Physics B: Atomic and Molecular Physics* 3.10 (1970): 1346.
- [23] McCall, B. J., et al. "Dissociative recombination of rotationally cold H 3+." *Physical Review A* 70.5 (2004): 052716.
- [24] Hjartarson, A. T., E. G. Thorsteinnsson, and J. T. Gudmundsson. "Low pressure hydrogen discharges diluted with argon explored using a global model." *Plasma Sources Science and Technology* 19.6 (2010): 065008.
- [25] Bogaerts, A., and R. Gijbels. "Modeling of metastable argon atoms in a direct-current glow discharge." *Physical Review A* 52.5 (1995): 3743.
- [26] Phelps, A. V. "Collisions of H+, H₂⁺, H₃⁺, ArH+, H-, H, and H₂ with Ar and of Ar+ and ArH+ with H₂ for energies from 0.1 eV to 10 keV." *Journal of physical and chemical reference data* 21.4 (1992): 883-897.
- [27] Hejduk, M. "Formation and Destruction of Para and Ortho H₃⁺ in Discharge and Afterglow. Experiments with Para-Hydrogen." WDS 2010-Proceedings of Contributed Papers. Proceedings of the 19th Annual Conference of Doctoral Students, held 1-4 June 2010, in Prague. Edited by Jana Safránková and Jirí Pavlů. Part II-*Physics of Plasmas and Ionized Media* (ISBN 978-80-7378-140-8) MATFYZPRESS, Prague, 2010., p. 54-59. 2010.
- [28] Karpasb, Z., V. Anicich, and W. T. Huntress Jr. "An ion cyclotron resonance study of reactions of ions with hydrogen atoms." *The Journal of Chemical Physics* 70.6 (1979): 2877-2881.
- [29] Fehsenfeld, F. C., A. L. Schmeltekopf, and E. E. Ferguson. "Thermal-energy ion—neutral reaction rates. VII. Some hydrogen-atom abstraction reactions." *The Journal of Chemical Physics* 46.7 (1967): 2802-2808.
- [30] Bruhns, H., et al. "Absolute energy-resolved measurements of the H→H→H₂+e- associative detachment reaction using a merged-beam apparatus." *Physical Review A* 82.4 (2010): 042708.
- [31] Harada, Nanase, and Eric Herbst. "Modeling carbon chain anions in L1527." *The Astrophysical Journal* 685.1 (2008): 272.
- [32] Rolin, M. N., et al. "Self-consistent modelling of a microwave discharge in neon and argon at atmospheric pressure." *Plasma Sources Science and Technology* 16.3 (2007): 480.
- [33] Zhu, Xi-Ming, and Yi-Kang Pu. "A simple collisional-radiative model for low-temperature argon discharges with pressure ranging from 1 Pa to atmospheric pressure: kinetics of Paschen 1s and 2p levels." *Journal of Physics D: Applied Physics* 43.1 (2009): 015204.
- [34] Bourene, M., and J. Le Calvé. "De-excitation cross sections of metastable argon by various atoms and molecules." *The Journal of Chemical Physics* 58.4 (1973): 1452-1458.
- [35] Sadeghi, N., and D. W. Setser. "Symmetry constraints in energy transfer between state-selected Ar*(3P₂, 3P₀) metastable atoms and ground state H atoms." *Chemical physics* 95.2 (1985): 305-311.
- [36] Dickerson, George Fielden. "A direct lifetime measurement for a resonance transition in argon." (1965).
- [37] Wiese, W. L., M. W. Smith, and B. M. Miles. Atomic transition probabilities. volume 2. sodium through calcium. *National Standard Reference Data System*, 1969.
- [38] Dose, V., and A. Richard. "Collision induced Lyman-alpha emission from metastable hydrogen." *Journal of Physics B: Atomic and Molecular Physics* 14.1 (1981): 63.
- [39] Glass-Maujean, M. "Collisional Quenching of H (2 S) Atoms by Molecular Hydrogen: Two Competitive Reactions." *Physical review letters* 62.2 (1989): 144.
- [40] Wiese, Wolfgang L., Melvin William Smith, and B. M. Glennon. Atomic transition probabilities. Volume 1. Hydrogen through neon. *National Bureau Of Standards Washington Dc Inst For Basic Standards*, 1966.
- [41] B. M. Smirnov, 2015. *Cham: Springer*, vol. 84